

# NUMERICAL SIMULATION OF TRANSPARENT GLASS-GFRP COMPOSITE BEAMS USING SMEARED CRACK MODELS

## **Luís VALARINHO**

Civil Engineer, M.Sc.  
IST / ICIST, Technical University of Lisbon,  
Av. Rovisco Pais, 1049-001, Lisboa, PORTUGAL  
*luis.valarinho@civil.ist.utl.pt\**

## **José SENA-CRUZ**

Assistant Professor, M.Sc., Ph.D.  
ISISE / University of Minho, Dept. of Civil Eng.  
Azurém, 4800-058, Guimarães, PORTUGAL  
*jsena@civil.uminho.pt*

## **João R. CORREIA**

Assistant Professor, M.Sc., Ph.D.  
IST / ICIST, Technical University of Lisbon,  
Av. Rovisco Pais, 1049-001, Lisboa, PORTUGAL  
*jcorreia@civil.ist.utl.pt*

## **Fernando A. BRANCO**

Full Professor, M.Sc., Ph.D.  
IST / ICIST, Technical University of Lisbon,  
Av. Rovisco Pais, 1049-001, Lisboa, PORTUGAL  
*fbranco@civil.ist.utl.pt*

## **Abstract**

This paper describes results of experimental and numerical investigations about the structural behaviour of composite beams made of annealed glass panes and GFRP pultruded profiles. A brief description of flexural tests previously carried out on glass and glass-GFRP composite beams is first presented. The second part of this paper describes the numerical simulation of a rectangular glass-GFRP composite beam. Two-dimensional finite element (FE) models of rectangular composite beams were developed in order to simulate and analyse their serviceability behaviour (prior to glass breakage) as well as their post-cracking behaviour until failure. To this end, a multi-fixed smeared crack model was used, and the effects of the following parameters were evaluated: (i) fracture energy of glass and (ii) shear retention factor. Experimental and numerical results are compared regarding the cracking load and post-cracking behaviour, namely in terms of crack pattern and load-deflection response.

**Keywords:** Adhesive bonding; Composite beams; Glass; GFRP; Numerical simulation; Parametric study; Smeared crack models.

## **1. Introduction**

In recent years there has been an increasing number of applications of glass in civil engineering structural elements, such as roofs, floors, beams and columns [1]. Such interest stems basically from the aesthetical possibilities of glass combined with its transparency. However, structural elements made of float glass present several limitations, including relatively low tensile strength and brittle behaviour, which contrasts with the current design philosophies associated with more conventional materials, such as steel and reinforced concrete, for which ductility of structural members must be guaranteed.

The traditional alternatives to overcome the above mentioned limitations of float glass consist of using either toughened glass or laminated glass [2]. Toughened glass presents higher tensile strength compared with float glass, however it still exhibits a fully brittle behaviour at failure. On the contrary, laminated glass is capable of displaying a pseudo-ductile and redundant behaviour – if one of its glass panes cracks or breaks, polyvinyl butyral (PVB) films not only keep them in place but also transfer the tensile stresses to the other panes.

More recently, a different approach has been pursued by several authors (e.g. [3-5]), which consists of joining glass panes to other structural materials, namely stainless steel, carbon fibre reinforced polymer (CFRP) laminates, concrete, wood and steel. The underlying principle of those composite members is similar to that of reinforced concrete and relies on the stress transfer between the glass pane and the strengthening material when the tensile stress of glass is attained.

Some studies have already addressed the numerical modelling of composite beams made of glass and different strengthening materials. Owing to the brittle material behaviour of glass, in order to avoid convergence problems, different simulation strategies have been used to handle glass cracking, including sequentially linear analysis (SLA) [4] and element “killing” [5]. In the former study, smeared crack models were used and, in order to avoid possible convergence problems stemming from the negative tangent stiffness of the softening law, the following two strategies were adopted: (i) incremental-iterative analysis was replaced by a series of scaled linear analyses; and (ii) the stress-strain softening law of glass was replaced by a “saw-tooth” reduction curve. Test data on stainless steel strengthened glass beams compared well with those obtained from numerical simulation and the effects of the following parameters were analysed: reduction steps of the “saw-tooth” curve; shear retention factor; and mesh size. In the later study, glass cracking was modeled by defining a failure criterion based on maximum principal strain which, when attained, causes a significant reduction of the material elasticity modulus.

This paper first describes the main results of an experimental programme about the structural behaviour of composite beams made of annealed glass panes and glass fibre reinforced polymer (GFRP) pultruded laminates. In this experimental campaign, described in detail in [6,7], flexural tests were carried out on glass and glass-GFRP composite beams, in which the effects of the geometry of the GFRP strengthening elements and the type of adhesive used to bond the strengthening elements to glass were investigated. The second part of this paper describes the numerical simulation of the beams tested. Two-dimensional finite element models were developed using FEMIX software [8], in order to simulate and analyse the serviceability behaviour of glass-GFRP composite beams (prior to glass breakage), as well as their post-cracking behaviour. A multi-fixed smeared crack model, available in FEMIX computer program, was used. For both investigations, numerical and experimental results are presented only for beams in which the strengthening material was bonded to the glass beam with an epoxy adhesive. This is related with the fact that, for now, the numerical models formulated are not capable of simulating a general adhesively bonded joint. For the beams bonded with epoxy, experimental studies showed that such adhesive was able to provide a high level of interaction at the bonded interfaces even for high load levels, which allows assuming complete interaction between the two materials in the numerical models. Experimental and numerical results are compared in terms of initial stiffness, cracking load and crack pattern.

## **2. Experimental investigations**

### **2.1 Structural concept**

A recent study carried out by the authors [6,7] showed the potential of using GFRP pultruded laminates bonded to the tensile edge of glass panes. This structural system, which resembles reinforced concrete, aims for highly redundant but transparent glass beams with increased post-cracking strength and ductility. Here, after glass breakage, the high strength and relatively low elasticity modulus of GFRP can be regarded as a relative advantage as it contributes to increase overall ductility when compared to other composite systems that have been suggested elsewhere. In the previous study conducted by the authors two structural systems, tested in bending in a simply supported configuration, were investigated: (i) beams with rectangular geometry, with a narrow GFRP laminate adhesively bonded to the bottom edge of the glass pane, acting as tensile reinforcement; and (ii) beams with wider GFRP laminates bonded to the top and bottom edges of a glass pane (web), acting as flanges of an I-section. Two types of adhesives (a stiff epoxy and a soft polyurethane) were used to bond the members of the glass-GFRP composite sections. Fig. 1 illustrates both geometries of beams produced with the epoxy adhesive.



**Figure 1: Glass-GFRP beams with rectangular (left) and I (right) cross-section.**

The results, summarized in this section, confirmed the potential of the structural system proposed, as GFRP strengthening provided considerable increase of both strength and ductility, with the structural performance of the composite system depending not only on the geometry of the strengthening element, but also on the mechanical behaviour of the adhesive. The results showed that composite beams with epoxy adhesive presented the highest values of cracking load and post-cracking load capacity. On the other hand, the composite beams with polyurethane adhesive presented the highest values of ductility, but exhibited much lower post-cracking load capacity. The different behaviour exhibited by beams made of the two different adhesives stemmed basically from the degree of shear interaction at bonded interfaces, which was complete with epoxy and partial with polyurethane. The remaining of this section describes in more detail results of the beam with rectangular geometry bonded with epoxy adhesive, as this was the one used for the numerical study.

## 2.2 Materials

Annealed glass panes (with edge treatment) with a thickness of 12 mm were used in the experiments. The ultimate strength and elasticity modulus of glass were determined through 4-point bending tests on small-scale glass specimens, carried out according to NP EN 1288-1:2007 and NP EN 1288-3:2007 standards and by means of flexural tests on full-scale glass beams, respectively. In those tests glass presented linear elastic behaviour until failure, with an ultimate tensile stress of  $\sigma_{u, \text{glass}} = 58.9 \pm 12.6$  MPa and an elasticity modulus of  $E_{\text{glass}} = 80.6$  GPa.

To strengthen the glass beam, a rectangular ( $12 \times 10$  mm<sup>2</sup>) GFRP pultruded laminate was used, which is made of an isophthalic polyester matrix reinforced with alternating layers of E-glass rovings and mats. The mechanical properties of the material were obtained from coupon tests, namely the axial ultimate tensile stress ( $\sigma_{u, \text{GFRP}} = 475.5 \pm 25.5$  MPa), the axial elasticity modulus in tension ( $E_{\text{GFRP}} = 32.8 \pm 0.9$  MPa) and the in-plane Poisson's ratio ( $\nu = 0.28$ ).

The GFRP laminate was bonded to the glass pane with an epoxy structural adhesive (Sikadur 330). The adhesive was tested in tension according to ISO 527-1:1993 and ISO 527-4:1997 standards and presented an initially linear behaviour with progressive loss of stiffness prior to failure, exhibiting an ultimate tensile stress of  $\sigma_{u, \text{epoxy}} = 22.5 \pm 3.9$  MPa and a tensile elasticity modulus of  $E_{\text{epoxy}} = 5.13 \pm 0.11$  GPa.

## 2.3 Geometry of the beams and test setup

A total of five beams, divided in two groups, were tested: (i) four glass beams, consisting of annealed glass panes (cross-section of  $12 \times 100$  mm<sup>2</sup>) and (ii) one composite beam, similar to the former, but strengthened in the bottom edge with the GFRP pultruded laminate (cross-section of  $12 \times 10$  mm<sup>2</sup>), adhesively bonded to glass with epoxy adhesive. All beams, with a 1.50 m span, were tested in 4-point bending configuration. The point loads were applied by means of an *Enerpac* hydraulic jack with a 100 kN load capacity connected to a steel loading

frame. A metal sphere was positioned between the hydraulic jack and a steel distribution beam to avoid any transverse loading. Two small rubbers were placed under the loaded sections in order to avoid direct glass-metal contact. All beam supports were materialized by means of 80 mm long steel plates placed on top of steel rollers with a 50 mm diameter. In both beams, in order to prevent lateral deformation, four pairs of vertical metal guides were symmetrically positioned throughout the span - the outer pairs were placed at the support sections while the inner pairs were 0.725 m apart themselves (see Fig. 1).

Load was measured using a *Novatech* load cell placed in-between the distribution beam and the hydraulic jack. Midspan deflections were measured with electrical *TML* displacement transducers, with strokes of 25 mm. On the composite beam, the axial strains throughout the depth of midspan section were measured with electrical *TML* strain gauges. All beams were monotonically loaded until failure under load control, at approximate speeds of 27 N/s and 10 N/s for the glass beams and the composite beam, respectively. The applied load, midspan deflection and axial strains were recorded in a PC, by means of an *HBM* data acquisition system at a speed of 1 Hz.

## 2.4 Results and discussion

Fig. 2 illustrates the load-midspan deflection curves of the tested beams (for glass beams, only one curve is plotted, which is representative of the remaining beams).

As expected, annealed glass beams presented linear behaviour up to failure, which was sudden and fragile, due to the development of a single crack (generally at the central part of the beam) that caused their collapse. The average failure load was 3.7 kN and the average deflection at failure was 2.92 mm (about  $L/514$ ,  $L$  being the span).

The load-deflection behaviour of the glass-GFRP beam was clearly different from that of the glass beams, especially after the development of the first visible crack, and it can be divided in two distinct stages separated by the moment when the first visible crack appeared. The initial behaviour of the composite beam was linear, with a slightly higher stiffness than that of the glass beams (1.44 kN/mm and 1.41 kN/mm, respectively). For a load of 4.8 kN, which is 29.7% higher when compared with the reference glass beam, a sudden and significant load reduction occurred, which was caused by the appearance of the first visible cracks in the glass. Contrarily to what was visible in the glass beam, the appearance of the first cracks did not cause the total collapse of the beam, but only a sudden decrease in the value of the applied load. The above mentioned cracks presented a regular pattern, with an almost vertical orientation and with a uniform spacing, and were confined to the central part of the beam. In a second stage, the load-deflection curve presents a set of linear segments, separated by smaller load decreases and with successive stiffness reductions associated to the development of the crack pattern. During this stage, the crack pattern is roughly similar to that exhibited by reinforced concrete beams: in the central part of the beam (with no shear force), the crack pattern kept its vertical orientation, while in the outer parts cracks started to incline towards the supports (see Fig. 3). Even after suffering successive load reductions, at the end of the tests the beam was still able to attain the maximum load reached in the first stage. The collapse of the composite beam was triggered by an almost horizontal shear crack in the glass pane, which was followed by the separation between the glass web and the GFRP laminate, next to one of the supports, for a midspan deflection of 13.8 mm (about  $L/109$ ).

Axial strains measured at different depths of the midspan section of the composite glass beam (for different load levels) showed that until glass cracking started the epoxy adhesive provided a complete interaction at the bonded interface. With the progressive development of cracks in the glass pane the axial strains in the GFRP strengthening element increased very significantly, showing that even for increasing load levels, the bonded connection was able to guarantee an adequate redistribution of stresses between the glass pane and the GFRP laminate.

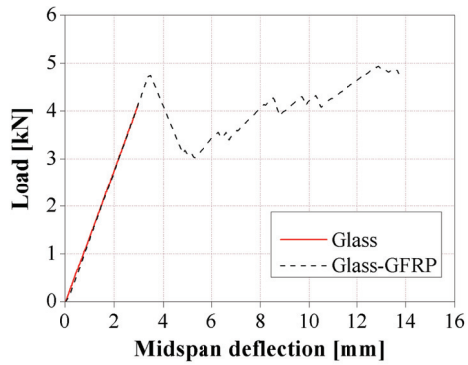


Figure 2 – Load vs. midspan deflection curves of the beams tested

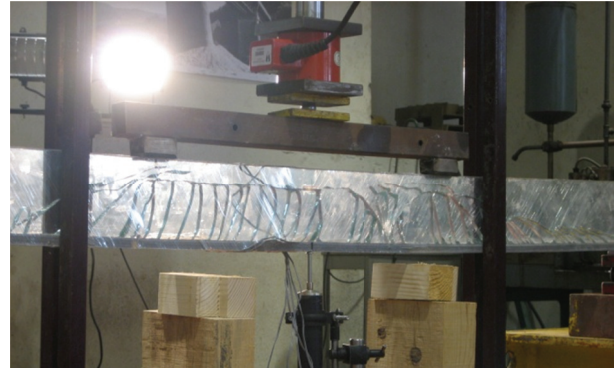


Figure 3 - Crack pattern in glass-GFRP composite beam.

### 3. Numerical simulation

#### 3.1 Initial considerations

Smearred crack models have been used for the simulation of concrete in tension since the 1970s. In these models, the fracture process is initiated when the maximum principal stress in a material point exceeds its tensile strength. The propagation of the cracks is mainly controlled by the shape of the tension-softening constitutive law and fracture energy of the material. Normally, the mesh objectivity is guarantee by associating the dissipated energy in crack propogation process with a characteristic length of the finite element. In order to avoid snap-back instability, the mode I fracture energy must be greater than a threshold value which depends on the tension-softening constitutive law. Typically, the fracture propagation in mode II is based on the concept of shear retention factor [9].

The numerical investigations described in this section comprised a parametric study carried out with the aim of evaluating the applicability of smeared crack models for the simulation of annealed glass structural elements. For that purpose a multi-fixed smeared crack model [9] was selected from the FEMIX computer code, which is a general tool for the analysis of structures by the Finite Element Method [8]. The main analysed parameters were the fracture energy and the shear retention factor.

#### 3.2 Description of the FE model

The strengthened beam was modelled as a plane stress problem. Fig. 4 shows the geometry, mesh, support conditions and load configuration used to develop the parametric study. To simulate the glass and GFRP, 4-node Serendipity plane stress elements were used with  $2 \times 2$  Gauss-Legendre integration scheme. Linear elastic behaviour under compression was adopted. Perfect bond was assumed between both materials. This assumption is corroborated by the experimental observations (see also Section 2). The shape of the tension-softening law was assumed as linear. The crack band width was assumed equal to the square root of the area of the finite element in order to assure that the results are not dependent on the mesh refinement. In the used multi-fixed smeared crack model, for a specific integration point, a new crack is initiated when the maximum principal stress exceeds the uniaxial tensile strength, and the angle between the direction of the existing cracks and the direction of the maximum principal stress exceeds the value of a predefined threshold angle. In the present study the threshold angle was assumed constant and equal to  $30^\circ$ . A maximum of 2 cracks per integration point was allowed to arise.

As referred before, the parametric study analysed the influence of the fracture energy and the shear retention factor on the relationship force vs. deflection at midspan. The numerical responses were compared with the experimental one. Additionally, in some cases the crack patterns were also compared.

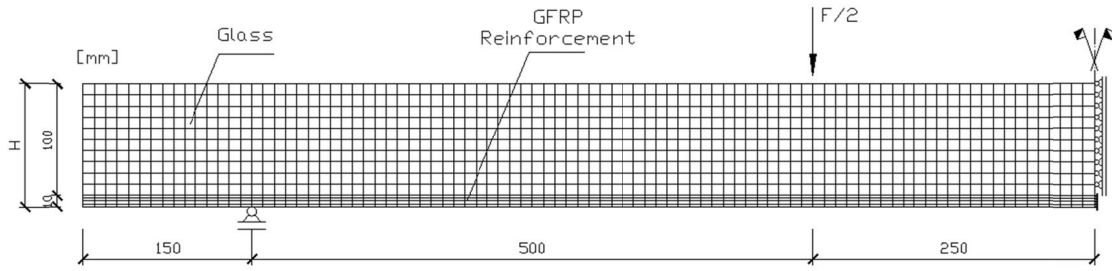


Figure 4 – Mesh, support conditions and load configuration.

### 3.3 Results and discussion

#### 3.3.1 Effect of fracture energy

For studying the effect of the mode I fracture energy ( $G_f$ ) on the structural response of the annealed glass beam strengthened with GFRP, the following values were considered:  $G_{f,min}$ ,  $1.5G_{f,min}$ ,  $2.0G_{f,min}$  and  $4.0G_{f,min}$ , where  $G_{f,min}$  is the minimum fracture energy required to avoid the snap-back instability [9]. According to the literature, the value of the glass fracture energy is about  $G_{f,min}/100$  [2], although to the authors' best knowledge there is no experimental work reporting the determination of such value ( $3 \times 10^{-3} \text{ J/m}^2$ ). It is also worth mentioning the considerable scatter of  $G_f$  reported in other more conventional materials, namely concrete, for which differences of the same order of magnitude have been reported by several authors [10]. In the simulations of the present section the parameter  $p$  defining the shear retention factor was assumed to be equal to 2.0 (see also section 3.3.3).

Fig. 5 depicts the relationships between the load and midspan deflection responses, both numerical and experimental. In this figure it can be seen that the simulation of the elastic branch matches the experimental response. With the exception of model “ $4.0G_{f,min}$ ” all the numerical models predicted the crack load initiation. After this point a sudden load decay is observed for the model “ $G_{f,min}$ ”. This load decay is similar to the one observed in the experimental test. However, when the corresponding deflection is compared a large difference can be observed. This difference can be attributed to the fact that the data acquisition of the experimental test may not have captured this drop since the adopted speed was 1 Hz. After this phase several cracks arose and then grew in terms of width and depth. At this stage, a similar response is observed for all the models (with the exception of model “ $4.0G_{f,min}$ ”), which predicted quite well the experimental response including the failure load.

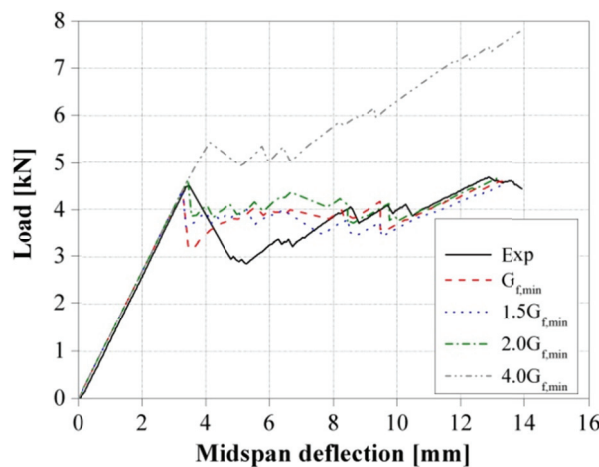


Figure 6 – Effect of fracture energy on the load vs. midspan deflection.

Fig. 8 presents the obtained crack patterns for different deflection levels of the models “ $G_{f,min}$ ” and “ $2.0G_{f,min}$ ”. For all the analysed stages, the existing cracks are mainly “fully opened” (in purple),

i.e. cracks where the mode I fracture energy is fully exhausted. In spite of model “ $2.0G_{f,min}$ ” predicted a greater number of flexural cracks with higher depth, the model “ $G_{f,min}$ ” showed a better similarity with the experimental observations in terms of crack pattern at the upper part of the strengthened beam. In addition of that, for both models, the horizontal cracks developing on the shear span at the GFRP vicinity can be perfectly identified in the experimental prototype.

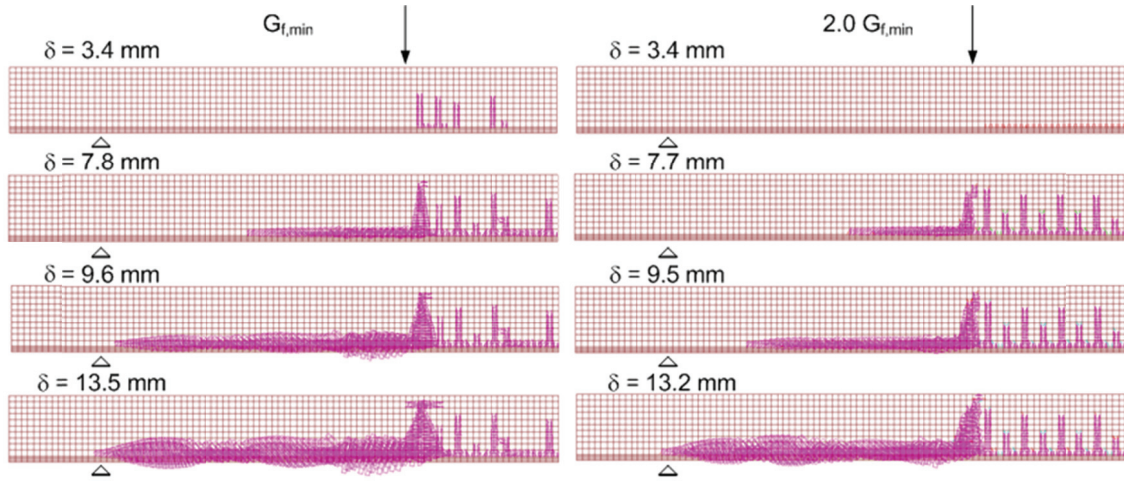


Figure 8 – Effect of the fracture energy on the crack pattern, for the models with  $G_{f,min}$  and  $2.0G_{f,min}$ .

### 3.3.2 Effect of shear retention factor

The nonlinear material model used allows the evaluation of the shear retention factor,  $\beta$ , in two distinct ways [9]: (i) a constant value; (ii) a non-constant value defined by  $\beta = (1 - \epsilon_{cr} / \epsilon_{cr,ult})^p$ , where  $\epsilon_{cr}$  and  $\epsilon_{cr,ult}$  are the crack normal strain and the ultimate crack normal strain, respectively, and  $p$  is a parameter that can assume the values of 1, 2 or 3. Figs. 7 and 8 show the influence of the shear retention factor on the structural response when the strategies (i) and (ii) are followed, respectively.

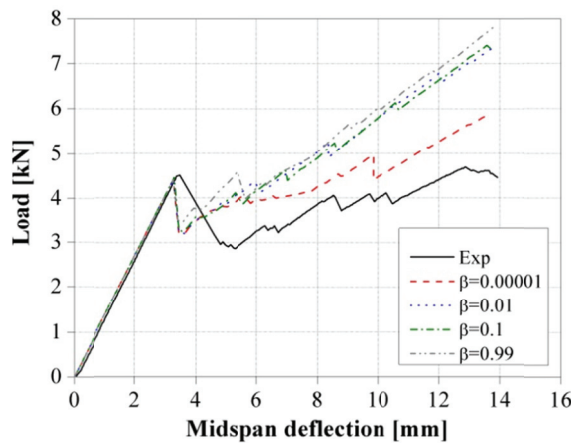


Figure 9 – Effect of shear retention factor on the load vs. midspan deflection.

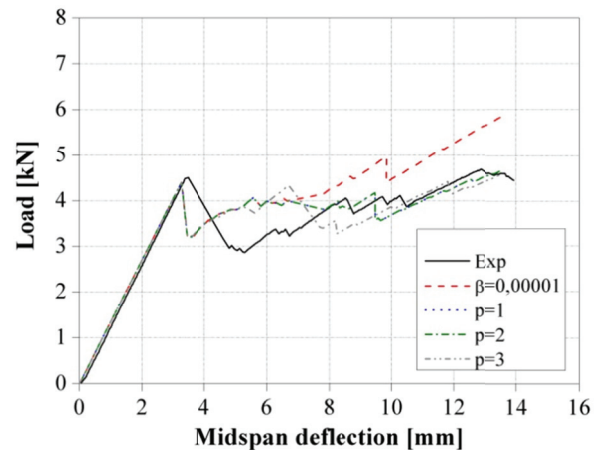


Figure 10 – Effect of the parameter  $p$  on the load vs. midspan deflection.

In these simulations a linear tension-softening constitutive law was used and the fracture energy was assumed equal to  $G_{f,min}$ . When a fixed value for  $\beta$  is assumed (see Fig. 7), after crack initiation, the numerical models overestimated the experimental result. This behavior was expected since during the crack propagation the numerical shear resistance degradation does not exist. When a non-constant value for the shear retention factor is adopted (see Fig. 8), the numerical model predicts quite well the overall response. Minimum differences were found for the case of  $p=1, 2$  and  $3$ .

## 4. Conclusions

This paper presented results of experimental and numerical investigations on composite structural beams that combine annealed glass panes and GFRP pultruded profiles, the later being used as strengthening elements and bonded to the former with epoxy adhesive. The following main conclusions are drawn:

- The main advantage of the composite beams proposed in this study is their post-cracking residual strength and ductility, and the experimental tests confirmed such better performance.
- A numerical parametric study was performed with a multi-fixed smeared crack model that includes a linear tensile-softening law. The fracture energy and the shear retention factor were the main parameters analysed.
- The model with the minimum fracture energy required to avoid the snap-back instability predicted with high accuracy the main aspects observed experimentally, such as the crack initiation, stiffness degradation, load carrying capacity and crack patterns.
- According to the studies performed, the shear retention factor cannot be constant during the numerical test in order to include the shear degradation.

## Acknowledgements

The authors wish to acknowledge FCT, ICIST and ADI (project n.º 3456/2009) for funding the research and companies SIKA, Guardian and STEP for having supplied the adhesives, the glass panes and the GFRP pultruded profiles used in the experiments.

## References

- [1] NIJSSE, R., “Glass in Structures”. Birkhäuser Publishers for Architecture, Basel, 2003.
- [2] HALDIMANN M, LUIBLE A, OVEREND M. “Structural Use of Glass”. Structural Engineering Documents 10, IABSE, Zurich, 2008.
- [3] LOUTER PC. “Adhesively bonded reinforced glass beams”, Heron 2007; 52: 31-58.
- [4] LOUTER C, VAN DE GRAAF A, ROTS J. “Modeling the Structural Response of Reinforced Glass Beams using an SLA Scheme”. In Proceedings of Challenging Glass 2, Conference on Architectural and Structural Applications of Glass (eds. Bos, Louter, Veer), Delft, The Netherlands, 2010.
- [5] ØLGARD AB, NIELSEN JH, OLESEN JF. “Design of mechanically reinforced glass beams: modelling and experiments”. Structural Engineering International 2009; 19(2): 130-136.
- [6] CORREIA JR, VALARINHO L, BRANCO FA. “Ductility and post-cracking strength of glass beams strengthened with GFRP pultruded composites”. Composite Structures 2011; 93(9): 2299-2309.
- [7] Valarinho L. “Construction in Structural Glass: Behaviour of Glass-GFRP Hybrid Beams”. M.Sc. Dissertation in Civil Engineering, IST-UTL, 2010 (*in Portuguese*).
- [8] SENA-CRUZ, J.M.; BARROS, J.A.O.; AZEVEDO, A.F.M.; VENTURA-GOUVEIA, A., “Numerical simulation of the nonlinear behavior of RC beams strengthened with NSM CFRP strips”. CMNE 2007 - Congress on Numerical Methods in Engineering and XXVIII CILAMCE - Iberian Latin American Congress on Computational Methods in Engineering, Abstract pp. 289, Paper nº 485 published in CD – FEUP, 20 pp., Porto, 13-15 June 2007.
- [9] SENA-CRUZ, J.M. “Strengthening of concrete structures with near-surface mounted CFRP laminate strips”. PhD Thesis, Department of Civil Engineering, University of Minho, 2004, 198 pp. URI: <http://hdl.handle.net/1822/11781>.
- [10] NETO, P.; ALFAITE, J.; ALMEIDA, J.R.; PIRES, E.B. “The influence of mode II fracture on concrete strengthened with CFRP”. Computers and Structures 2004; 82(17-19): 1495-1502.